Engineering and Computational Mechanics
Volume 166 Issue EM3

Clearing effects on plates subjected to blast loads
Rigby, Tyas, Bennett, Warren and Fay

ice | proceedings

Proceedings of the Institution of Civil Engineers
Engineering and Computational Mechanics 166 September 2013 Issue EM3
Pages 140–148 http://dx.doi.org/10.1680/eacm.12.00010
Paper 1200010
Received 11/07/2012 Accepted 14/01/2013
Keywords: computational mechanics/dynamics/mathematical modelling

ice Institution of Civil Engineers publishing

Clearing effects on plates subjected to blast loads

Sam E. Rigby MEng
PhD Student, University of Sheffield, Sheffield, UK

Andrew Tyas MEng, PhD
Reader in Blast & Impact Engineering, University of Sheffield, Sheffield, UK; Technical Director, Blastech Ltd, Sheffield, UK

Terry Bennett MEng, PhD
Senior Lecturer in Computational Mechanics, University of Sheffield, Sheffield, UK

James A. Warren MEng, PhD
Laboratory Principal, University of Sheffield, Sheffield, UK; Managing Director, Blastech Ltd, Sheffield, UK

Stephen Fay MEng
Research Engineer, Blastech Ltd, Sheffield, UK

Empirical prediction methods are often used in the early stages of design to quantify the blast load acting on a structure. While these methods are reasonably accurate for geometrically simple scenarios, they may not be accurate for situations where the target does not form a reflecting surface of effectively infinite lateral extent. In this case, the blast wave will diffract around the target edge, leading to the propagation of a relief wave inwards from the edge of the structure, reducing the late-time development of pressure in a process known as 'clearing'. This paper presents results from a study undertaken to determine the influence of clearing on the response of simple targets. Experiments were conducted in which deflection–time histories were recorded for target plates subjected to cleared and non-cleared blast loads. These were compared with predictions from explicit dynamic finite-element and single-degree-of-freedom models, in which the blast loading was derived by applying a simple correction to the empirical blast prediction method. The results presented show that neglecting clearing may result in highly conservative predictions of target response and that analyses using loading derived from simple corrections to the ConWep predictions match the experimentally observed results very closely.

Notation

a	sonic velocity in air
a_0	sonic velocity in air (at ambient conditions)
C_D	drag coefficient
d	plate thickness
E	elastic modulus of target
f	natural frequency
K_L	load transformation factor
K_M	mass transformation factor
k	stiffness of target
L	span
p_r	reflected overpressure
p_{so}	incident overpressure
q	dynamic pressure
R	range from charge centre (stand-off)
S	target front face height or half-width (smallest value)
T	natural period
t	time
t_c	clearing time
t_d	positive phase duration
W	explosive mass
x	shortest distance from a point on a target to the nearest free edge
Z	scaled distance ($R/W^{1/3}$)
$z_{max,1}$	peak displacement after first quarter cycle
δ	Hudson's time scale
η	Hudson's clearing length scale
ν	Poisson's ratio of target
ρ	density of target

1. Introduction

When designing a structure to resist a blast load, an accurate description of the temporally varying pressure acting on the target is required before the performance of the structure can be assessed. While complex numerical analyses can be undertaken at this stage, it is often preferable for an engineer to use approximate tools for determining the loads that will arise from a predetermined blast event. This is particularly used in the early stages of design, where these approximations can readily give an indication of the damage a target is likely to sustain before more complex analyses are undertaken.

The empirical 'look-up' method of Kingery and Bulmash (1984) (hereby called the KB method) is well-established and implemented in the computer code ConWep (Hyde, 1991). This method provides a simple means for predicting the blast pressure at any scaled distance, $Z = R/W^{1/3}$ between 0·067 and 39·67 kg/m$^{1/3}$, where R is the distance from the point of interest to the charge centre (called the 'range' or 'stand-off') and W is the mass of explosive, expressed as an equivalent mass of TNT. While this method may be attractive for simple scenarios, a more refined approach is usually required when the geometry of the target will

influence the late-time development of pressure on the loaded face. A fundamental assumption of the KB method is that the reflecting surface is effectively infinite in lateral extent; if this is not the case, then blast wave clearing will occur.

When a propagating blast wave reaches the edge of a target, there is an instantaneous imbalance between the reflected pressure, p_r, acting on the loaded face and the lower magnitude incident pressure, p_{so}, acting in the region outside the target, immediately adjacent to the target edge. As a result of this pressure imbalance, flow is established as the pressure begins to equalise. As the blast wave diffracts around the edge of the target and the high-pressure gas vents into the lower pressure region, a rarefaction wave beings to travel inwards along the loaded face. The rarefaction 'relief' wave sweeps in from the edges of the target and acts to reduce the pressure acting at any point that the wave propagates over. This process, known as 'clearing', is known to significantly reduce the impulse acting on the target face, as has been shown both experimentally (Rickman and Murrell, 2007; Rose *et al.*, 2006; Smith *et al.*, 1999; Tyas *et al.*, 2011) and numerically (Rose and Smith, 2000; Rose *et al.*, 2006; Shi *et al.*, 2007).

Current design guidance (e.g. US DoD, 2008) provides only basic measures for including blast wave clearing in the design of structural elements. While Rickman and Murrell (2007) offer an improved methodology for predicting the pressure acting on a target based on curves fit to a series of experimental traces and Rose and Smith (2000) present a series of empirical 'clearing factors' to adjust the impulse acting on a target based on the results of numerical analyses, there was, until recently, no known approach for predicting clearing that was founded on fundamental physical principles.

In fact, just such a method has been presented in an entirely overlooked study by Hudson (1955). This approach approximated the rarefaction clearing wave as an acoustic pulse and derived clearing functions that could be superimposed on the full reflected pressure–time history – determined, for example, from the KB empirical load model – to give accurate predictions of the pressure acting at any point on a finite target subjected to a cleared blast wave. Hudson's predictions were confirmed by Tyas *et al.* (2011) who showed that they provided extremely good predictions of temporally varying pressure loads on targets with small lateral dimensions recorded in carefully controlled experiments.

In the current study, previous work by the authors on determining a temporally varying load on an effectively rigid target is expanded to determine the effect of clearing on deformable structures. A series of experimental and numerical trials was conducted on test plates situated in

(*a*) an effectively infinite reflected surface, where the plate will experience the full 'non-cleared' pressure load
(*b*) a finite reflecting surface, where blast wave clearing will influence the late-time pressure acting on the target and the plate will experience a 'cleared' pressure load.

Measuring the displacement of the test plates allows the influence of clearing to be isolated and quantified, with experimental data available for validation of the numerical model. The purpose of this paper is to demonstrate the influence that blast wave clearing has on the dynamic response of plates subjected to blast loads and to show that predictions of blast wave clearing can be implemented into simple design methods to accurately predict the deformation of finite targets.

2. Predicting blast wave clearing

Empirical predictions for the onset of clearing relief, such as the method presented by Kinney and Graham (1985), only attempt to correct the total impulse acting on the loaded face, and not the temporal or spatial distribution of cleared pressures. This method assumes that clearing relief acts uniformly over the whole loaded face, beginning immediately at the time of arrival of the blast wave and decaying linearly thereafter. Clearing is said to be complete once the overpressure reaches the stagnation pressure – given as the sum of the incident pressure, $p_{so}(t)$, and drag pressure, $C_D q(t)$ – and is said to follow the stagnation pressure for the remaining duration of the load. The time it takes for clearing to be complete (i.e. when the cleared pressure reaches stagnation pressure) is known as the clearing time, t_c, and is given by Kinney and Graham (1985) as $t_c = 3S/a$, where S is the height or half-width of the front face (whichever is smaller) and a is the sonic velocity in the reflected region.

While this method has its clear advantages – it is a simple correction and the resulting spatially uniform pressure can be readily used in single-degree-of-freedom (SDOF) analyses (Biggs, 1964) – its physical validity is questionable (Rickman and Murrell, 2007) and the assumption that clearing relief begins immediately cannot be valid for a point remote of the free edge; there will be some transient time before the clearing wave arrives and the point of interest will experience no clearing relief until then (Tyas *et al.*, 2011).

2.1 The Hudson method

Hudson (1955) presented the spatial and temporal distribution of a clearing relief wave caused by the impingement of a planar blast wave on a rigid target, approximating the rarefaction wave as an acoustic pulse. This method is based on the assumptions that the shock is weak (i.e. although the clearing wave travels through shocked air, it is acceptable to assume that it propagates at the ambient sonic velocity), the blast wave is planar (i.e. the lateral dimensions of the target are small in comparison to the stand-off, R) and the depth of the target is sufficiently large to ensure that no clearing waves arrive from the back face during the duration of loading. Given these assumptions, the acoustic approximation can be used to determine the pressure acting at any point on the target face, giving full spatial and temporal distribution of the cleared blast pressure.

Hudson (1955) presents the contours of relief pressure (normalised against the peak incident overpressure) in terms of non-dimensional length and time parameters. Hudson's non-dimensional length scale, η, is given as

$$\eta = x/a_0 t_d \quad (1)$$

where x is the distance from the point of interest to the nearest free edge, a_0 is the sonic sound speed in air (assumed to be 340 m/s) and t_d is the positive phase duration. Hudson's time scale, δ, is given as

$$\delta = t/t_d - \eta \quad (2)$$

where t is time. Figure 1 shows the temporal and spatial distribution of the clearing relief wave. For any point on a target, $0 < \eta < 1$ ($\eta = 0$ indicates a point on the free edge whereas $\eta \geqslant 1$ indicates a point that will experience the full reflected pressure for the entire duration of the positive phase), the time-varying pressure associated with the clearing wave can be evaluated and superimposed with the reflected pressure acting on the target to determine the cleared pressure at that point. This method has been shown to be in excellent agreement with experimentally measured pressure traces (Tyas *et al.*, 2011) and provides a simple yet physically robust method for determining the pressure acting on a target whose reflecting surface cannot be assumed to be infinite.

3. Experimental study

In order to quantify the response of flexible structural targets subjected to cleared and non-cleared blast loading, a series of small-scale experimental trials was undertaken at the University of Sheffield Blast & Impact Lab., Buxton, UK. Hemispherical PE4 charges (with a TNT equivalence of 1·2) were placed 6 m away from a reinforced concrete bunker wall that contained a steel plate lined porthole (320 × 305 mm clear dimensions) into which the non-cleared test plate was located. The minimum distance from the test plate to a free edge of the bunker wall was at least 4 m. The positive phase durations of the hemispherical charges used in this work were all less than 3 ms – a clearing wave travelling at 340 m/s from the nearest free edge would take >11·5 ms to reach the target before it could begin to affect the loading on the target, hence the reflecting surface can be assumed to be effectively infinite in lateral extent.

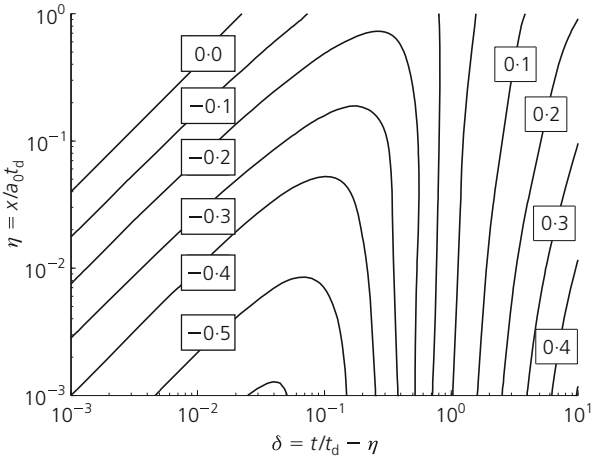

Figure 1. Spatial and temporal properties of the rarefaction relief wave (Hudson, 1955). Contours of clearing relief are given as $p/p_{so,max}$ and Hudson's length and time scale (η and δ) are given in Equations 1 and 2

Orthogonal to the bunker wall, 6 m away from the centre of the explosive, a test plate was located within a finite reflecting surface, comprising a rigid block with dimensions such that the target would experience cleared loading. The depth of the target block was >2 m, ensuring no clearing waves would arrive from the back of the target. The experimental setup, shown in Figure 2, enabled the dynamic deflection of plates subjected to cleared and non-cleared blast loads to be measured and the influence of clearing to be quantified.

The test plates were 0·835 mm thick mild steel. Non-cleared test plates were located in a 305 mm wide, 320 mm high porthole

(a)

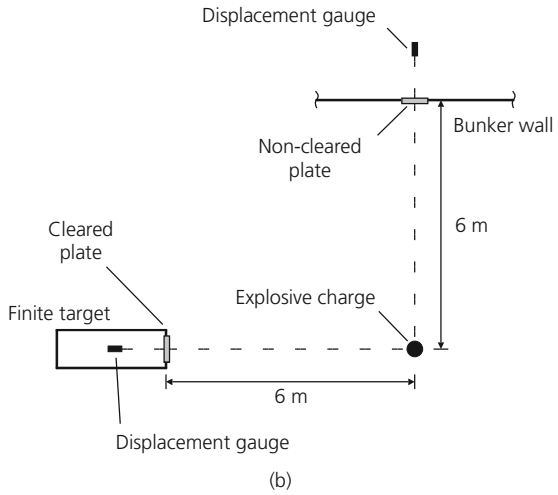

(b)

Figure 2. (a) General arrangement of the test arena and (b) schematic illustration of test setup

that had been cut in the bunker wall, 305 mm above ground level. The target block was a 600 mm square by 1·8 m long reinforced concrete block clad in 15 mm thick steel plate to provide a flat regular surface. An additional steel frame, fabricated from 15 mm steel plate, was attached to the front, providing housing for the laser displacement gauge. A porthole was cut into the front of the steel frame, with the same dimensions as the porthole in the bunker wall, at the same height above the ground surface. The test plate in the finite surface was located along the vertical centreline of the front face of the target block, with 238·5 mm either side to the edges of the reflecting surface and 65 mm to the top. Dimensions of the finite target are shown in Figure 3.

A clamping plate was attached to the front of both finite and infinite targets using $8 \times$ M10 bolts; this was used to constrain rotation at the supports while the bolt holes in the test plates were oversized, allowing free horizontal translation. Additionally, molybdenum grease was liberally applied to the faces of the porthole and clamping frames, which were in contact with the target plate in order to minimise in-plane resistance at the supports. The plates were one-way spanning (horizontally spanning the 305 mm) and were slightly undersized in the vertical dimension to allow the top and bottom edges to translate freely without striking the porthole frame.

Deflection was measured by M7 laser distance sensors (bandwidth of 10 kHz and resolution accuracy of $\pm$0·6 mm) manufactured by MEL Microelektronik GmbH. Displacement data were recorded using a TiePie Handyscope 4 digital oscilloscope, recording samples at 312·5 kHz and 14 bit resolution. Recording was triggered by the failure of a break-wire wrapped around the detonator in order to synchronise records with the time of detonation. The hemispherical charges were detonated using electronically activated L2A1 detonators.

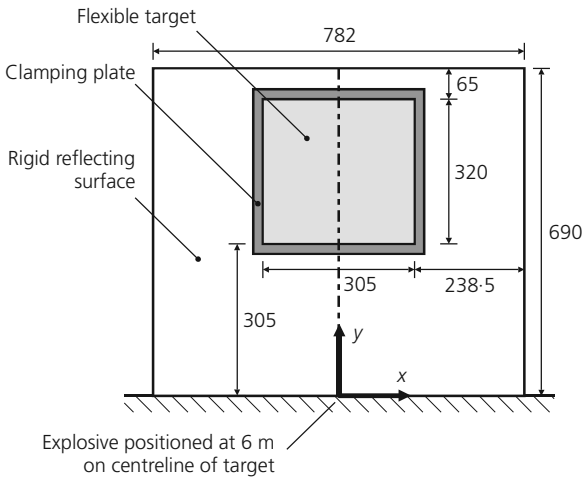

Figure 3. Dimensions of the finite reflecting surface (dimensions in mm)

The experimental trials were conducted with hemispherical PE4 charges ranging from 50 to 175 g, with the stand-off set at 6 m throughout. Five charge masses were tested, with one repeat test per charge mass. In each test, the displacements of the cleared and non-cleared plates were measured, giving a total of 20 test results. A summary of the test plan is shown in Table 1.

4. Numerical modelling

Numerical analyses were performed using the explicit finite-element code LS-DYNA (Hallquist, 2006). The plate was discretised into a grid of 64×64 Belytschko–Tsay shell elements with four integration points through the thickness of the shell. The mesh size was chosen based on the results of a preliminary mesh sensitivity study.

The plate was modelled as a linear elastic material with elastic modulus $E = 210$ GPa, density $\rho = 7850$ kg/m^3 and Poisson's ratio $\nu = 0{\cdot}3$ as the plates were expected to deform in the elastic range throughout. The boundary conditions of the plate were chosen to match those in the experimental work – that is, along the two vertical faces the plate was constrained against rotation and against translation perpendicular to the plane of the plate, but was free to translate in-plane. The horizontal edges were unrestrained.

When performing numerical analyses of structures subjected to blast loads, the explosion detonation and subsequent shock wave propagation can be modelled explicitly within a Eulerian or arbitrary Lagrangian–Eulerian (ALE) air domain. The load is then transmitted to the Lagrangian solid structure via fluid–structure interaction (FSI); however, this process often results in computationally expensive models (Slavik, 2009) that can be unsuitable for use in the early stages of design.

An alternative and commonly used approach is to determine the blast load from some other analysis (such as the empirical approaches described in Section 1) and then apply this to the structural members as load curves. The simplest versions of this approach ignore FSIs and reflections/shielding from obstacles adjacent to the target of interest, although these factors can be included by factoring the blast load magnitude to allow for target compliance (Kambouchev *et al.*, 2007; Teich and Gebbeken,

Test	*W*: g (PE4)	*R*: m	*Z*: m/kg$^{1/3}$
1, 2	50	6	15·3
3, 4	75	6	13·4
5, 6	108	6	11·9
7, 8	140	6	10·9
9, 10	175	6	10·1

Table 1. Summary of charge masses *W* and stand-offs *R* used in experimental trials. A TNT equivalence of 1·2 was assumed for PE4

2012) and/or using a ray-tracking approach to consider reflections and obstructions, as for example in the Blast-X code (Britt and Lumsden, 1994).

In the current study, shielding and reflection were unimportant and the effect of target compliancy was considered to be negligible given the short duration of loading relative to the period of the test panels. Load curves were therefore generated using two of the simplest and most commonly used blast load generation codes – the *Load_Blast loading module in the LS-DYNA finite-element code (based on the ConWep implementation of the KB load model (Randers-Pehrson and Bannister, 1997)) and the Loads on Structures module (LOS) of the ConWep code (Hyde, 1991). *Load_Blast allows for arbitrary target geometries, while LOS is confined to rectangular targets normal to the shock front. LOS also purports to include load reduction due to clearing, although these predictions have been shown to be grossly inaccurate when compared to data from carefully controlled experimental tests (Rickman and Murrell, 2007; Tyas *et al.*, 2011).

In the DYNA numerical study, the plates were analysed under two loading options – *Load_Blast applied to the non-cleared plates and the KB reflected pressure with Hudson corrected load applied to the cleared plates. The load was applied to the cleared plates as separate force–time functions at each node in the following way.

(*a*) The full reflected pressure–time history, given the charge mass and stand-off, was applied to every node. It was assumed that the shock front arrived at every node simultaneously and was assumed to be uniform in magnitude (i.e. slant distance and angle of incidence effects were ignored). With a scaled target height of 0·5 m/kg$^{1/3}$ at a scaled distance of $>$10·0 m/kg$^{1/3}$ this is a reasonable assumption to make – the peak pressure and time of arrival, given by ConWep LOS, differ by no more than 1% across the plate.
(*b*) For each node, the distance x to the free edge enabled the Hudson clearing length, η, to be evaluated for each node (Equation 1). The corresponding pressure–time function (Figure 1) given by the Hudson method was applied to each node with identical x coordinates (32 node sets, given symmetry about the vertical axis). The coordinate system is shown in Figure 3.
(*c*) The clearing relief wave corresponding to the distance to the vertical free edge of the target was applied to each node with identical y coordinates (65 node sets).
(*d*) Each node was therefore subjected to the superposition of three load curves – the reflected pressure and x and y components of clearing relief (the pressure was multiplied by the element area to give a load–time history).

A total of 98 load curves were defined for the 4225 nodes and were generated using a purpose-written Matlab pre-processor. Numerical analyses were performed for all five charge masses, with separate runs for Hudson and *Load_Blast loading options. Hudson's clearing length scale (η, Equation 1) changes with positive phase duration, hence the Hudson clearing functions were evaluated for each charge mass separately. Damping was not included in the numerical model as it could not be accurately quantified for the target and is likely to make little difference to the first quarter cycle of displacement (i.e. to first peak deflection).

Figure 4 shows the pressure predictions from a 75 g PE4 charge at 6 m. ConWep predictions for reflected pressure show the typical load that the non-cleared plate was subjected to in tests 3 and 4, and Hudson predictions for the furthest and nearest points from the free edge of the finite target give an indication of the range of pressures acting on the cleared plate. For the point in the bottom-centre of the target, (0, 0·305), the clearing lengths associated with the x and y distances to the free edge are 0·48 and 0·49 respectively; clearing waves from the top and sides arrive approximately half way through the positive phase. For the top corners of the plate, (0·15, 0·625) and (−0·15, 0·625), the x and y clearing lengths are 0·08 and 0·30, and the clearing waves can be seen to arrive much earlier; the clearing wave from the top face arrives 0·2 ms after load application.

SDOF analyses of the plates were also undertaken in order to assess how accurately a simple analytical approach could predict the experimentally observed plate deflections. The following four load cases were modelled.

(*a*) 'Cleared' – reflected positive and negative pressures with Hudson clearing corrections. The spatially varying load was transformed into an equivalent uniform load using the spatial load factor derived by Rigby *et al.* (2012).
(*b*) 'Non-cleared' – full reflected positive and negative phase

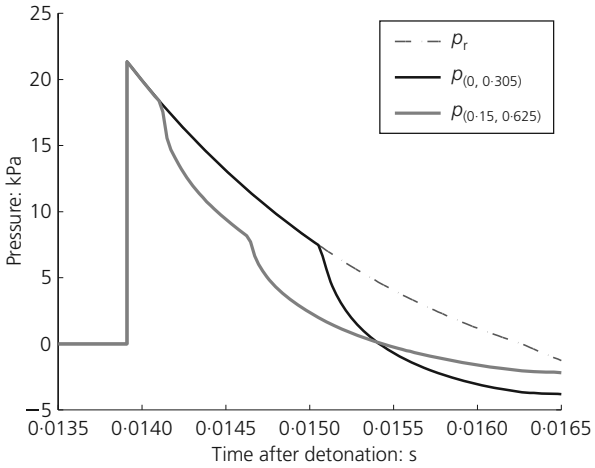

Figure 4. Reflected pressure (p_r) and clearing pressure acting at the furthest ($p_{(0, 0·305)}$) and nearest ($p_{(0·15, 0·625)}$) points from the free edge for a 75 g PE4 charge at 6 m

pressure applied as a uniform load with no clearing corrections. For the two load cases above, positive phase parameters were given by the KB empirical method and negative phase pressures were given using the relationship from Granstrom (1956).

(*c*) 'ConWep' – the equivalent uniform impulse, given by ConWep LOS, applied as a triangular pulse (the peak overpressure was preserved and the load duration reduced to maintain the impulse). This takes into account ConWep clearing predictions.

(*d*) 'Linear' – a triangular pulse with peak reflected pressure and positive impulse given for the full reflected case. This does not include clearing and is typically used as a first stage in design. For the two load cases above, the negative phase is neglected.

The plates were modelled as fully clamped, elastic one-way spanning beams with no in-plane translational restraint at the supports. The SDOF properties of the plate are shown in Table 2, where the load factor and mass factor are used to transform the distributed properties of the target into the equivalent properties of the single-degree system (Biggs, 1964).

5. Results and discussion

5.1 The influence of clearing

Displacement–time histories for tests 4, 8 and 9 are shown in Figure 5 for the first ~10 ms of response. In the numerical model, the load was applied at time $t = 0$ and the displacements were time-shifted to correspond with the beginning of the experimental displacements – in all cases, this was never more than ±50 μs from the arrival time predicted by ConWep.

In all three tests shown, the influence of blast wave clearing is apparent. For the plates embedded within a finite reflecting surface, the reduction in late-time pressure and total impulse associated with blast wave clearing is enough to significantly lessen the response of the target.

The simple assumption that clearing reduces the overpressure to the sum of the incident and drag pressure is clearly not valid for short duration blast events. In Figure 4 (the predicted pressure acting on the plates in tests 3 and 4), the cleared pressures become negative (below atmospheric) across the whole plate at

Span, L	305 mm
Thickness, d	0·835 mm
Load factor, K_L	0·53
Mass factor, K_M	0·41
Elastic stiffness, k	$384EI/L^3$
Natural frequency, f	47·5 Hz
Natural period, T	21·0 ms

Table 2. Dynamic properties of the plate used in the SDOF analysis

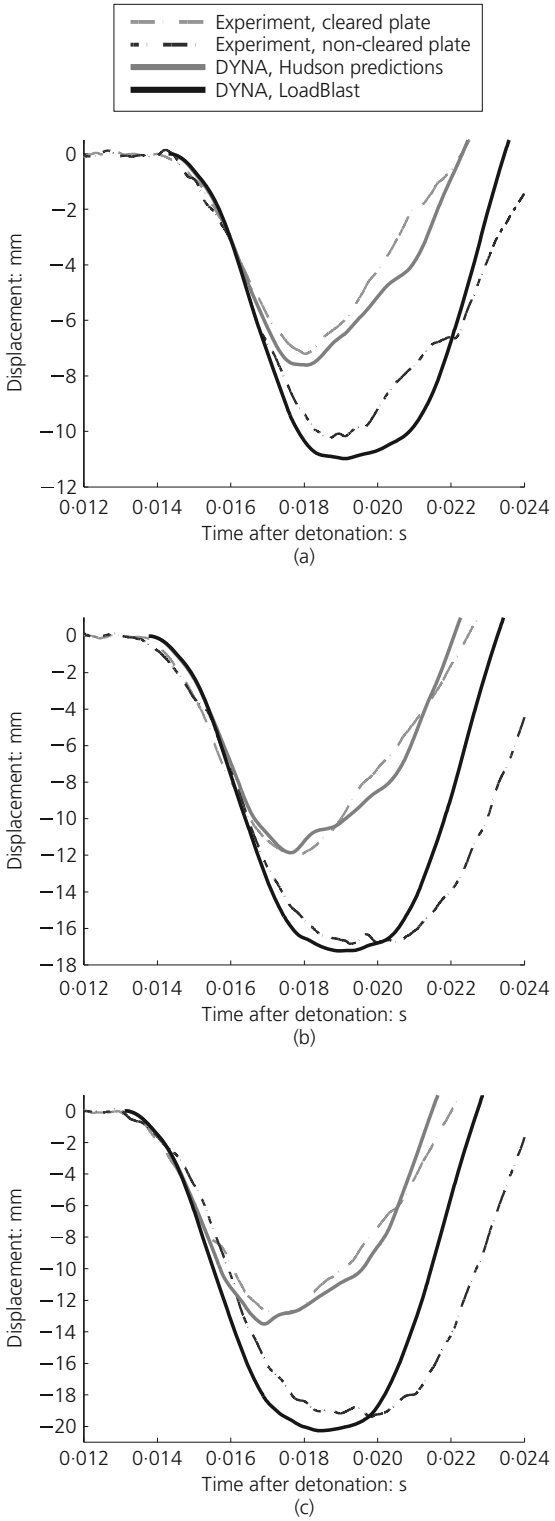

Figure 5. Experimental and numerical results for steel plates subjected to cleared and non-cleared blast loads: (a) test 4, 75 g; (b) test 8, 140 g; (c) test 9, 175 g

around 15·4 ms after detonation. These early negative pressures occur when the plate is still displacing away from the blast, and serve to decelerate the cleared plate. Coupled with a reduced positive phase impulse, this results in significantly lower values of displacement. It can be seen in Figure 5(a) that the response of the cleared and non-cleared plates begins to diverge around 16 ms after detonation. This behaviour was observed for all tests and is accurately captured by the numerical model.

The peak displacement after the first quarter cycle, $z_{max,1}$, is an indicator of the likely damage that a target will sustain from a high explosive blast. Values of $z_{max,1}$ for all experimental and numerical tests are shown in Figure 6. When the blast wave is free to clear around the edges of the finite target, the peak displacement is between 64 and 71% of the non-cleared peak displacement.

The Hudson method allows the pressure acting on a finite target to be predicted accurately (Tyas *et al.*, 2011) and can be readily implemented into commercial finite-element software. This enables the deflection of finite targets to be evaluated while retaining the simplicity and low computational cost of a purely structural analysis. Table 3 shows the absolute values of peak displacement ($z_{max,1}$) for all trials, as well as the percentage difference between experimental and numerical results. In a study on simplified blast tools, Bogosian *et al.* (2002) conclude that ConWep predictions best represented the blast parameters (i.e. peak pressure, impulse and duration) for the range of test results collected. The findings from the present study confirm that, if the target is embedded in an infinite reflecting surface, *Load_Blast can predict the peak displacement to within 7% of the experimental results. This simple numerical method can be used to gain a first approximation of the typical response characteristics and peak displacement of plates subjected to blast loads. With smaller targets, however, neglecting clearing can lead to over-conservative estimations and the need to accurately model blast wave clearing becomes apparent.

Test	*W*: g	$\lvert z_{max,1}\rvert$					
		Cleared			Non-cleared		
		Exp.	Num.	% diff.	Exp.	Num.	% diff.
1	50	5·4	5·8	8	8·2	8·2	0
2	50	5·2	5·8	13	8·1	8·2	1
3	75	7·3	7·6	4	10·3	11·0	7
4	75	7·2	7·6	6	10·3	11·0	7
5	108	9·1	9·9	8	13·8	14·3	3
6	108	9·5	9·9	4	13·7	14·3	4
7	140	11·3	11·9	5	16·8	17·2	3
8	140	12·0	11·9	−1	16·9	17·2	2
9	175	12·9	13·5	5	19·4	20·3	4
10	175	12·6	13·5	7	19·5	20·3	4

Table 3. Comparison of peak displacements, $z_{max,1}$, for numerical and experimental trials

If the target is not embedded in an infinite surface, a simple adjustment to the reflected pressure curve using the Hudson method can predict the peak displacement to within 13% of the experimental values. In situations where the centre of the charge is far from the target and the blast wave is unobstructed between the detonation point and the target, then the low computational cost and demonstrated validity of the Hudson predictive method should be preferred over more complex schemes.

5.2 Single-degree-of-freedom response

The results of the SDOF analyses for peak displacement on the first bounce, $z_{max,1}$, are shown in Figure 7, along with the experimental results for reference. Table 4 shows the absolute values of peak displacement for the SDOF analyses.

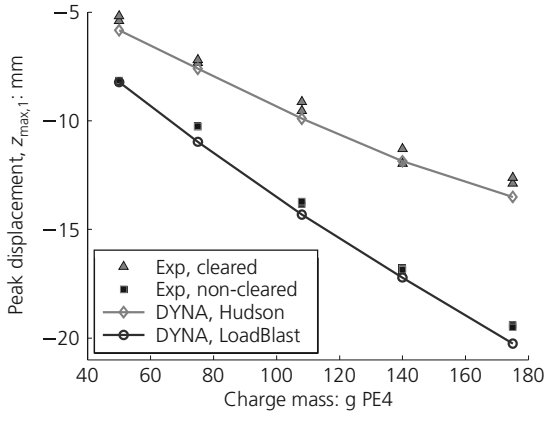

Figure 6. Experimental and DYNA peak displacements after the first quarter cycle, $z_{max,1}$

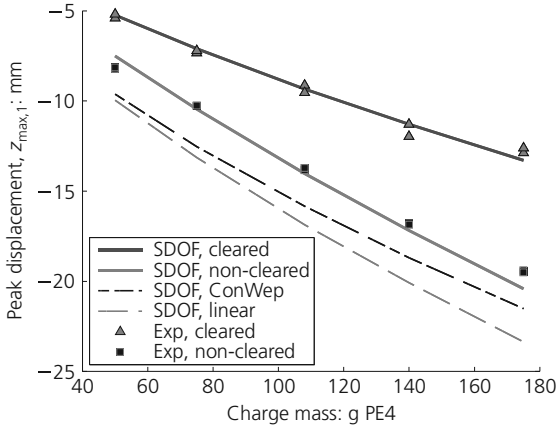

Figure 7. Experimental and SDOF peak displacements after the first quarter cycle, $z_{max,1}$

W: g	$\lvert z_{max,1} \rvert$			
	Cleared	Non-cleared	ConWep	Linear
50	5·2	7·5	9·6	10·0
75	7·1	10·5	12·5	13·1
108	9·3	14·0	15·8	16·9
140	11·3	17·2	18·7	20·1
175	13·3	20·4	21·5	23·4

Table 4. Peak displacements, $z_{max,1}$, for SDOF analyses

If the load is modelled as a linear pulse with the full positive phase impulse, the SDOF overestimates the peak deflection of the non-cleared plates. The ratio of load duration to natural period is roughly 0·1; the loading is highly impulsive and, particularly with far-field loading, inclusion of the negative phase for impulsive analyses is important (Teich and Gebbeken, 2010). When the load is modelled as a full positive and negative phase pressure, the inclusion of the negative phase enables the SDOF model to predict the peak response of the non-cleared plates to a sufficient level of accuracy. When the Hudson load model is used to account for clearing, the SDOF model is again able to predict the peak response of the cleared plates to a high level of agreement with the experimental results. Figure 8 shows the displacement–time histories for tests 9 and 10 and the SDOF model under the cleared load; the natural period of the plate and the peak displacement are accurately predicted. This highlights the validity of the SDOF method for use in simple scenarios and shows the ability of the Hudson method to be implemented into simple numerical models.

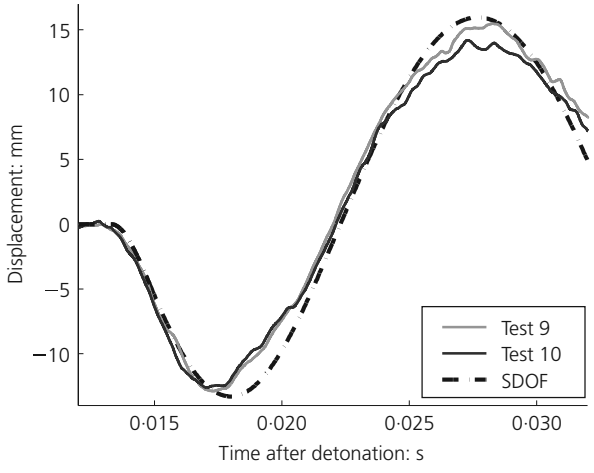

Figure 8. Experimental and SDOF displacement–time history for cleared plates subjected to 175 g PE4 (tests 9 and 10)

6. Conclusions

This work has comprised carefully controlled experimental investigations of the temporal deflection of simple elastic plates subjected to cleared and non-cleared blast loading, together with associated explicit dynamic finite-element and SDOF modelling. This work was conducted both to provide information to quantify the effect of clearing on structural response and to assess the accuracy of modelling using loading by different prediction methods.

The results show that, for the scenarios considered, clearing can have a significant effect on reducing the first peak deflection. Although the target response in this work was kept within the elastic realm for simplicity, it is likely that similar, if not more pronounced, differences between cleared and non-cleared deflections would be seen if the target response was non-linear. This strongly implies that ignoring clearing effects may be significantly over-conservative.

The modelling results using simple load curves with and without the inclusion of clearing effects showed excellent correlation with the experimental deflection–time and peak deflection data. This indicates that using load curves derived from simple empirical predictive methods and the application of the Hudson clearing correction can be used with confidence in modelling, as long as the limiting assumptions of the Hudson approach are valid. Strikingly, the SDOF analyses with and without cleared loading corrections were in excellent agreement with the experimental data, giving confidence that this approach is suitable for initial analyses of loading events for geometrically simple scenarios.

The dimensionless formulation of the Hudson approximation enables clearing to be evaluated for a wide range of scaled distances, explosive masses and target sizes that may be of interest to engineers, providing the assumptions of a weak shock front and planar blast are acceptable. When considering far-field loading, where clearing cannot be neglected, damage to light cladding and glazing could be significant. The predictive load model explored in this study may assist engineers in efficiently designing such systems, while still retaining the benefits of simplicity and low computational cost of an already well-established design approach.

Acknowledgement

The first author acknowledges financial support from the Engineering and Physical Sciences Research Council (EPSRC) for a doctoral training grant.

REFERENCES

Biggs J (1964) *Introduction to Structural Dynamics*. McGraw-Hill, New York, NY, USA.

Bogosian D, Ferritto J and Shi Y (2002) Measuring uncertainty and conservatism in simplified blast models. *Proceedings of the 30th Explosives Safety Seminar, Atlanta, GA, USA*, 1–26.

Britt JR and Lumsden MG (1994) *Internal Blast and Thermal Environment from Internal and External Explosions: A User's Guide for the BlastX Code, Version 3.0*. Science Applications International Corporation, St. Joseph, LA, USA, Technical report SAIC 405-94-2.

Granstrom S (1956) *Loading Characteristics of Air Blasts from Detonating Charges*. Royal Institute of Technology, Stockholm, Sweden, Technical report 100.

Hallquist JO (2006) *LS-DYNA Theory Manual*. Livermore Software Technology Corporation, Livermore, CA, USA.

Hudson C (1955) *Sound Pulse Approximations to Blast Loading (with Comments on Transient Drag)*. Sandia Corporation, Maryland, USA, Technical report SC-TM-191-55-51.

Hyde D (1991) *Conventional Weapons Program (ConWep)*. US Army Waterways Experimental Station, Vicksburg, MS, USA.

Kambouchev N, Noels L and Radovitzky R (2007) Numerical simulation of the fluid–structure interaction between air blast waves and free-standing plates. *Computers & Structures* **85(11–14)**: 923–931.

Kingery C and Bulmash G (1984) *Airblast Parameters from TNT Spherical Air Burst and Hemispherical Surface Burst*. US Army BRL, Aberdeen Proving Ground, MD, USA, Technical report ARBL-TR-02555.

Kinney G and Graham K (1985) *Explosive Shocks in Air*. Springer, New York, NY, USA.

Randers-Pehrson G and Bannister K (1997) *Airblast Loading Model for DYNA2D and DYNA3D*. US Army Research Laboratory, Aberdeen Proving Ground, MA, USA, Technical report ARL-TR-1310.

Rickman DD and Murrell DW (2007) Development of an improved methodology for predicting airblast pressure relief on a directly loaded wall. *Journal of Pressure Vessel Technology* **129(1)**: 195–204.

Rigby SE, Tyas A and Bennett T (2012) Single-degree-of-freedom response of finite targets subjected to blast loading – the influence of clearing. *Engineering Structures* **45**: 396–404.

Rose T and Smith P (2000) An approach to the problem of blast wave clearing on finite structures using empirical procedures based on numerical calculations. *Proceedings of the 16th Symposium on the Military Aspects of Blast and Shock (MABS16), Oxford, UK*, 113–120.

Rose TA, Smith PD and May JH (2006) The interaction of oblique blast waves with buildings. *Shock Waves* **16(1)**: 35–44.

Shi Y, Hao H and Li ZX (2007) Numerical simulation of blast wave interaction with structure columns. *Shock Waves* **17(1–2)**: 113–133.

Slavik TP (2009) A coupling of empirical explosive blast loads to ALE air domains in LS-DYNA. *Proceedings of the 7th European LS-DYNA Users Conference*, Salzburg, Austria.

Smith PD, Rose TA and Saotonglang E (1999) Clearing of blast waves from building facades. *Proceedings of the Institution of Civil Engineers – Structures and Buildings* **134(2)**: 193–199.

Teich M and Gebbeken N (2010) The influence of the underpressure phase on the dynamic response of structures subjected to blast loads, *International Journal of Protective Structures* **1(2)**: 219–234.

Teich M and Gebbeken N (2012) Structures subjected to low-level blast loads: analysis of aerodynamic damping and fluid–structure interaction. *Journal of Structural Engineering* **158(5)**: 625–635.

Tyas A, Warren J, Bennett T and Fay S (2011) Prediction of clearing effects in far-field blast loading of finite targets. *Shock Waves* **21(2)**: 111–119.

US DoD (US Department of Defence) (2008) *Structures to Resist the Effects of Accidental Explosions*. US DoD, Washington, DC, USA, UFC 3-340-02.